Sains Malaysiana 50(11)(2021): 3373-3382
http://doi.org/10.17576/jsm-2021-5011-21

Preparation of Nano-Iron Loaded Cassava Fibre Composite Material for Hexavalent Chromium Removal

(Penyediaan Bahan Komposit Serabut Ubi Kayu Terisi Nanozarah Besi untuk Penyingkiran Kromium Heksavalen)

HAOBIN SHI, WENBIN ZHANG, FENG CHEN, QINGSHENG SHI, FEI CHEN, LI FU* & SHICHAO ZHAO

ABSTRACT

Waste cassava fiber and tea polyphenols were used as carrier materials and reducing agents, respectively, to prepare nano-iron loaded cassava fiber composite (CF-FeNPs). This work investigated the factors affecting the removal of Cr(VI) by CF-FeNPs under different environmental conditions and the removal mechanism. The SEM characterization results show that as the initial Fe^{2+} concentration increases, the amount of nano-iron on the surface of the composite material increases. The results show that the increases of the initial Fe^{2+} content and dosage of CF-FeNPss can enhance the removal rate. Meanwhile, the decrease of the initial concentration of Cr(VI) solution and pH also beneficial for the removal performance. When pH=2.0 and the initial concentration of Cr(VI) is 10 mg/L, the removal rate of hexavalent chromium by CF-FeNPs can reach 81.4% within 2 h. The reaction conforms to the pseudo first-order kinetic model. The results of this study can provide technical reference for the remediation and treatment of Cr(VI)-containing wastewater.

Keywords: Nanocomposite; pollution control; removal mechanism; tea polyphenols; wastewater

ABSTRAK

Sisa serabut ubi kayu dan polifenol telah digunakan sebagai bahan pembawa dan agen penurun masing-masing untuk menghasilkan komposit serabut ubi kayu terisi nanozarah besi (CF-FeNPs). Penyelidikan ini mengkaji faktor yang mempengaruhi penyingkiran ion Cr(VI) oleh CF-FeNPs) pada keadaan persekitaran yang berbeza serta mekanisme penyingkiran. Pencirian menggunakan SEM menunjukkan bahawa peningkatan kepekatan Fe^{2+} telah meningkatkan kandungan nanozarah besi yang terbentuk pada permukaan komposit. Keputusan menunjukkan bahawa peningkatan kepekatan Fe^{2+} telah meningkatkan kadar penyingkiran Cr(VI). Pada pH=2.0 dan kepekatan awal Cr(VI) 10 mg/L, penyingkiran Cr(VI) boleh mencapai setinggi 81.4% dalam masa 2 jam. Tindak balas ini berpadanan dengan model kinetik tertib pertama pseudo. Keputusan kajian ini boleh menjadi rujukan teknikal bagi kajian rawatan air buangan yang mengandungi Cr(VI).

Kata kunci: Air buangan; kawalan pencemaran; komposit nano; mekanisme penyingkiran; polifenol teh

INTRODUCTION

Cr(VI) is a highly toxic heavy metal with high mobility and is difficult to be reduced by microorganisms. It is easy to accumulate in organisms through the food chain. Once it is discharged, it will bring lasting disasters to the environment (Dong et al. 2016). Therefore, Cr(VI) is considered to be one of the most harmful chemical substances to the human body, and is listed as one of the most toxic pollutants by the United States Environmental Protection Agency (USEPA) (Wang et al. 2017). Chromium mainly exists in the form of Cr(VI) and Cr(III) in nature (Fu et al. 2013), among which Cr(VI) has strong mobility and is more toxic, which is 100 times that of Cr(III) (Zeng et al. 2019). Exposure to Cr(VI) is likely to cause carcinogenesis, teratogenesis and mutagenesis, and has serious damaging effects on people and the environment (Clementino et al. 2018). Therefore, removing Cr(VI) in polluted wastewater is the key to ensuring water quality and safety. Cr(VI) is a priority control pollutant among environmental metal pollutants (Fu et al. 2019; Karimi-Maleh et al. 2021a, 2021b; Zhou et al. 2020). At present, the repair methods for Cr(VI) pollution in water bodies

mainly include chemical methods (such as chemical reduction method (Dermentzis et al. 2012), electrolysis method (Qian et al. 2014), photocatalysis method (Sun et al. 2019)), physical methods (such as adsorption (Wei et al. 2013), ion exchange (Kalidhasan et al. 2013), membrane separation (Koushkbaghi et al. 2018)) and biological method (microbial remediation) (Batool et al. 2012), and plant adsorption (Banerjee et al. 2018). These methods have certain limitations, therefore, seek an environment friendly and quick response method is imperative.

Nano iron particles (FeNPs) have been widely used in the field of environmental remediation due to their unique physical and chemical properties, large specific surface area and high reactivity (Chen et al. 2017; Jing et al. 2016). Traditional nano-iron is usually prepared by high-energy ball milling (Wang et al. 2020), liquid-phase reduction (Bae et al. 2016) or pyrolysis of carbonyl iron (Kumar et al. 2018). However, the general physical methods have higher requirements for the equipment and the FeNPs morphology control ability is limited. They also include strong reducing agent (sodium borohydride or hydrazine hydrate) which is toxic and will cause environmental issues. In addition, the high surface energy of nanoparticles will cause oxidation and agglomeration, which reduces the reactivity.

The use of plant extracts as a reducing agent to synthesize iron nanoparticles as a green chemical technology with fast response, non-toxic, and environmentally friendly (Chavan et al. 2020). The use of plant extracts to synthesize nano iron can make full use of the active ingredients in natural plants to reduce the agglomeration problem of FeNPs due to its own magnetism with stable physical and chemical properties (Ebrahiminezhad et al. 2018). Machado et al. (2013) selected 26 plant leaf extracts to prepare FeNPs with a particle size of 10-20 nm. The results showed that the antioxidant properties of oak leaves, pomegranate leaves and green tea were relatively optimal. Wang et al. (2014) compared the FeNPs prepared from the eucalyptus leaf extract with the FeNPs synthesized by the traditional method. The degree of agglomeration of eucalyptus leaf-based FeNPs is smaller and it is easier to store stably.

Tea leaf can be used for synthesizing by FeNPs due to its rich in antioxidants such as tea polyphenols, theaflavins, gallic acid, and flavonoids. These molecules can also effectively remove free radicals from the human body and inhibit the formation of active oxygen (Gautam et al. 2018). Huang et al. (2014) compared the performance of FeNPs prepared from green tea, oolong tea, and black tea. When green tea is used, the iron content is the highest, the size is the smallest, and the specific surface area is the largest. The degradation efficiency of malachite green can reach more than 80%. The authors believe that this may be related to the higher content of polyphenols and caffeine in green tea. Ghanim et al. (2020) synthesized of FeNPs using black tea leaves extract as adsorbent for removing eriochrome blue-black B dye. It is reported that the toxicity of FeNPs obtained by reducing nitrate with tea polyphenols in tea extract is lower than that obtained when borohydride is used as a reducing agent (Plachtová et al. 2018).

The agglomeration of nanomaterials is an important issue for reducing performance. By introducing a substrate to support nanomaterials, the agglomeration of FeNPs can be reduced while maintaining the high reactivity. At the same time, this strategy can also enhance its stability and oxidation resistance, and improve the recovery rate. At the same time, the substrate also has a certain adsorption effect, which improves the ability of FeNPs to remove pollutants. According to reports, traditional substrate materials include: chitosan, silica, kaolin, zeolite, bentonite, clay, ion exchange resin and activated carbon (Mashayekhi et al. 2018). Considering the popularization and use of FeNPs in groundwater and soil environmental remediation, it is imperative to seek a substrate material with high economic and environmental benefits.

Cassava fiber is one of the main agricultural wastes obtained during the production of cassava starch. It has a large output with high processing cost. The large number of dumping will cause many environmental problems. In view of this, this article aims to make secondary comprehensive utilization of cassava fiber. In this study, FeNPs was loaded on low-cost cassava fiber to prepare FeNPs composite material for removing Cr(VI) in water. Tea polyphenols used as reducing agents can well prevent the agglomeration between FeNPs. This composite has a good catalytic degradation effect. This composite showed a good catalytic degradation effect. The optimum performance was studied by exploring the comparing of different factors such as FeNPs composites prepared by different initial Fe^{2+} concentrations, pH, dosage and the initial Cr(VI) concentration. The morphology of the prepared FeNPs composite was characterized by SEM. The mechanism of composite for removing Cr(VI) from water was carried out as well. This work aims to provide a theoretical basis for the preparation of FeNPs composite and its application in environmental remediation.

Materials and Methods

The Cr(VI) solution used in the experiment is a national standard sample (1000 μg/L) (Zhang et al. 2017). Tea polyphenol (99%), ferrous sulfate ($FeSO_4 \cdot 7H_2O$, AR) and diphenyl semicarbazide ($C_{13}H_{14}N_4O$, AR) were purchased from Macleans Reagent Co., Ltd. Acetone (C_3H_6O, AR), sulfuric acid (H_2SO_4, GR) and phosphoric acid (H_3PO_4, AR) were purchased from Sinopharm Chemical Reagent Co., Ltd. Anhydrous ethanol (CH_3CH_2OH, AR) was purchased from Hangzhou Gaojing Fine Chemical Co., Ltd. The experiment uses deionized water. Cassava Fiber (CF) was taken from Zhejiang Huaxin Agricultural Biotechnology Co., Ltd. The cassava fiber was dried in a blast drying box at 60 °C for 12 h and then cooled. The fiber then ground to obtain cassava fiber powder. The CF powder was placed in a drying container for use.

10 g/L tea polyphenols (TP) solution was slowly added dropwise to 0.4 M $FeSO_4$ solution, under the condition of magnetic stirring at room temperature. After the reaction for 2 h, the black solid (FeNPs) was obtained by centrifugation, which was washed twice with deionized water and ethanol solution. When the tea polyphenol solution was added to the ferrous sulfate solution, the solution gradually changed from light blue-green to indigo blue and then to black, indicating the formation of FeNPs suspension, as shown in Figure 1.

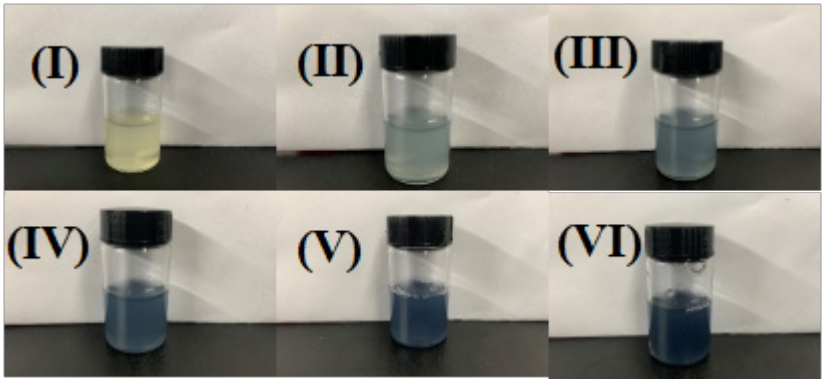

FIGURE 1. The process of ferrous sulfate solution when slowly add tea polyphenols solution (I) - (VI)

Fifty mg of cassava fiber powder was added into $FeSO_4$ solution of the same concentration and magnetically stir at room temperature for 8 h. Then, 10 g/L tea polyphenol solution was added dropwise, react under magnetic stirring for 2 h and centrifuge to obtain black solid powder (CF-FeNPs), and washed twice with deionized water and ethanol solution. After drying these two materials in an oven, the sample was collected at room temperature after grinding for later use.

A batch experiment was used to determine the efficiency of CF, FeNPs, and CF-FeNPs in removing Cr(VI) in aqueous solution. CF, FeNPs, and CF-FeNPs were added into a 40 mL sample bottle. Then, 10 mg/L (20 mL) of Cr(VI) solution was added under stirring at a constant speed (250 r/min) and a constant temperature (25 °C). 0.1 M H2SO4 has been used to adjusts the pH of the solution. Sample has been taken at regular intervals and immediately filtered using a 0.22 μm membrane filter, and then measured the residual chromium in the solution. All experiments were performed in duplicate, and the results were averaged.

An ultraviolet-visible spectrophotometer (759-UV1600, Shanghai, China) was used to determine the concentration of Cr(VI) at 540 nm using the diphenyl semicarbazide method (Janghel et al. 2007). The morphology of different materials was characterized by SEM.

The Cr(VI) removal efficiency of CF-FeNPs composite material is expressed by the following equation:

$$R(\%) = \frac{(C_0 - C_e)}{C_0} \times 100\%$$

where C_0 and C_e are the initial and equilibrium liquid phase concentrations of Cr(VI), respectively.

Kinetic analysis of reaction between composite materials and Cr(VI) is a complex reaction that occurs on the surface of the material. The pseudo-first-order

kinetic equation simplifies the Langmuir-Hinshelwood first reaction kinetic model. The equation is as follows:

$$\ln(\frac{C_t}{C_0})=-k_{obs}t$$

where $\ln(C_t/C_0)$ has a linear relationship with t; k_{obs} is the apparent rate constant; C_t is the concentration at time t; and C_0 is the initial concentration.

Results and Discussion

Figure 2 shows the morphology of CF, FeNPs, and CF-FeNPs. Figure 2(a) shows the CF with a rough morphology. Figure 2(b) shows the FeNPs prepared using tea polyphenols as a reducing agent. FeNPs are mainly spherical with spherical nodules. The particle size is between 80-150 nm. The FeNPs are constructed by a polyphenol polymer network. Figure 2(c)-2(f) are CF-FeNPs composites prepared under different concentrations of ferrous sulfate (0.1M-0.4M). With the increase of precursor concentration, the number of attached nanoparticles can be obviously observed in CF-FeNPs composites. The loaded FeNPs mainly exist in the form of spheres compounded into popcorn shape. The originally rough surface of CF becomes smooth as well. Since the polyphenol-iron polymerization network produced during the reaction covers the surface of CF, the number of agglomerations is greatly reduced compared to pure FeNPs. Compared with previous reports, the FeNPs loaded on the CF showed a much uniform size (Mehrotra et al. 2017; Yin et al. 2021).

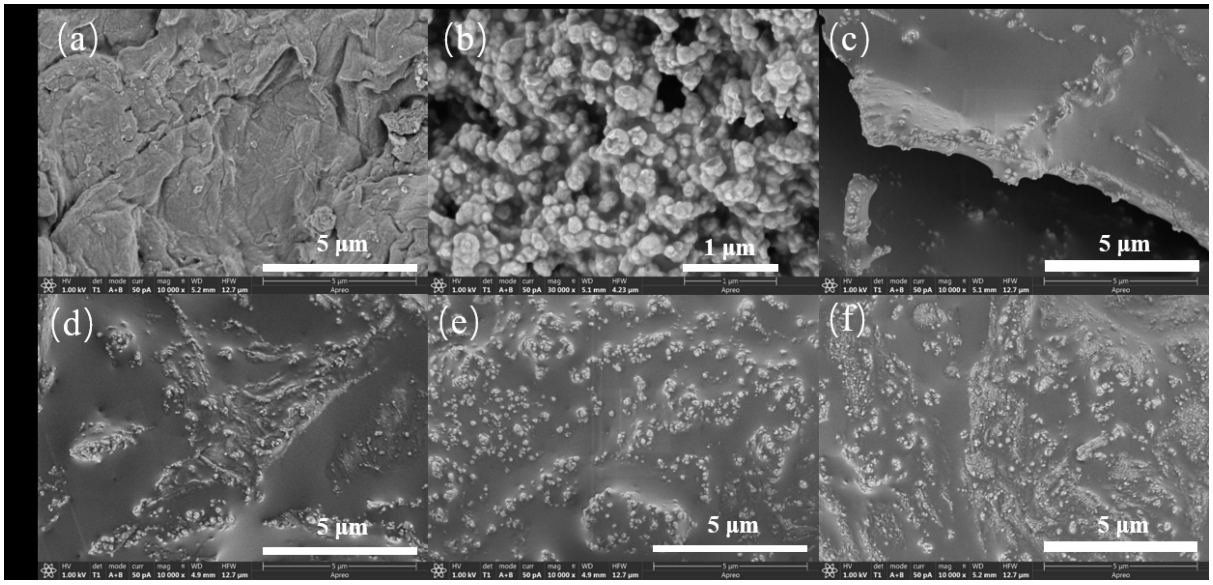

FIGURE 2. SEM images of (a) cassava fiber; (b) synthetic FeNPs; and (c) ~ (f) CF-FeNPs synthesized under different concentrations of precursor (0.1M-0.4M)

First, we studied the adsorption effect of different materials on hexavalent chromium. Figure 3 shows the removal efficiency of CF, FeNPs, and CF-FeNPs for Cr(VI) in aqueous solution. The removal efficiency of CF can only reach about 9% after 2 h. As a kind of plant fiber, CF can adsorb Cr(VI) on the fiber surface through physical adsorption. By using pure synthetic FeNPs, the removal efficiency is slowly increased from 24.7% in 15 min to 62.3% in 4 h. FeNPs have a reducing effect on metal ions and surface adsorption and complexation. The slow increase in removal efficiency may be due to the aggregation of FeNPs. When CF is used as the supporting substrate to load FeNPs, the removal rate is increased to 67.3% in 2 h and 81.4% in 4 h, which is much higher than the removal efficiency of ordinary cassava fiber and synthetic FeNPs.

Due to the improvement of the Cr(VI) removal efficiency of CF-FeNPs composite materials, we further studied the effect of CF-FeNPs prepared with different concentrations of precursor on the removal of Cr(VI). The

results are shown in Figure 4(a), the removal efficiency of CF-FeNPs for Cr(VI) only reached 42.4% and 54.3% in 4 h, using 0.1 M and 0.2 M precursor, respectively. This is a significant improvement in the removal efficiency of CF, but it is 20% and 8% less than pure FeNPs. This indicates that when the Fe^{2+} concentration increases, the removal efficiency of Cr(VI) will also increase due to the increase in the number of FeNPs loaded on the surface of the prepared composite material. When the concentration of ferrous sulfate gradually increased to 0.3 M, the removal efficiency of Cr(VI) reached 66.4% within 4 h, which was comparable to the removal efficiency of bare FeNPs. As the concentration further increased to 0.4 M-0.5 M, the removal efficiency of CF-FeNPs for Cr(VI) reached 81.4% and 80.9% within 4 h, respectively. In summary, we chose 0.4 M for the preparation of CF-FeNPs.

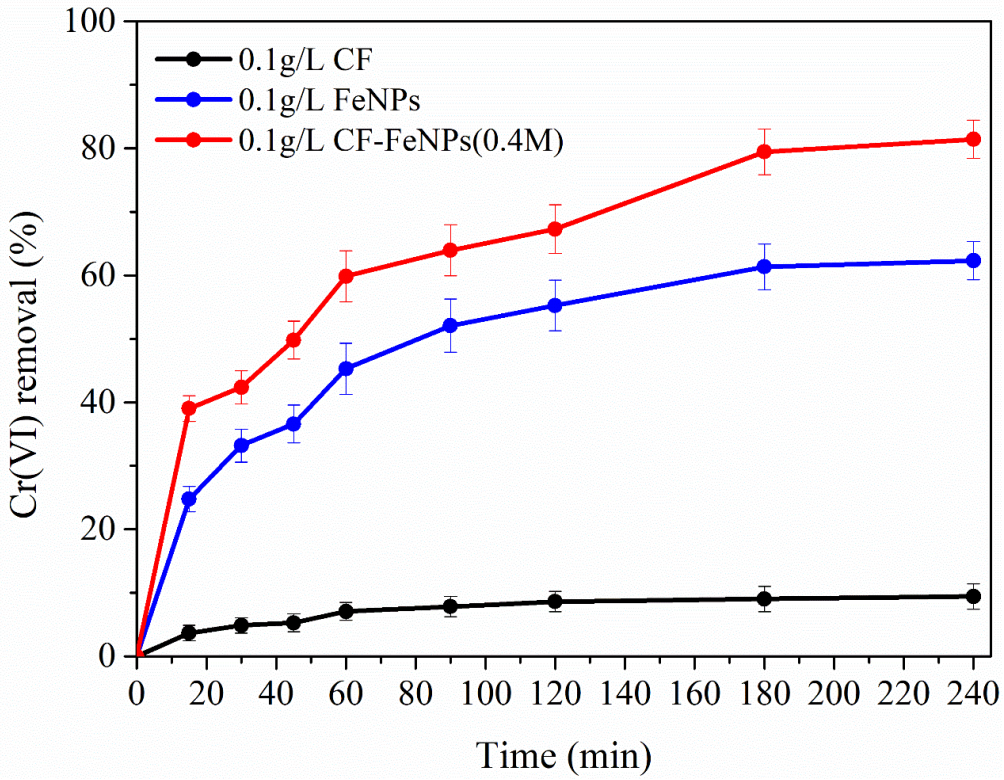

FIGURE 3. The effect of different materials on the removal of Cr(VI) (initial Cr(VI) concentration is 10 mg/L, Fe^{2+} concentration is 0.4 M, CF-FeNPs dosage is 0.1 g/L, pH=2.0, n=3)

As an important environmental factor, pH has a great influence on the adsorption reaction and the reduction of zerovalent iron (Patel et al. 2020). The lower the pH, the more conducive to the dissolution of iron, and more Fe^{2+} is generated, which helps the pollutants react on the surface of FeNPs. In addition, under weakly acidic conditions, the surface of FeNPs is more likely to be positively charged. Electrostatic attraction makes it easier for the negatively charged anions CrO_4^{2-}/ CrO_7^{2-} have contact reactions on the surface, thereby promoting the reduction of Cr(VI). When pH<6.5, Cr(VI) mainly exists in the form of $HCrO_4^-$ (Mohan & Pittman Jr. 2006), and iron mainly exists in the form of Fe^{2+} and Fe^{3+}. Figure 4(b) shows the removal effect of CF-FeNPs on Cr(VI) at pH=2, 3, 4, 5, 6. With the decrease of pH, the removal efficiency of Cr(VI) by CF-FeNPs increased significantly. When pH=2, the removal rate after 4 h can reach 81.4%, while when pH=6, the removal rate after 4 h is only 30.2%. The reaction equation of nano-iron and Cr(VI) is as follows:

$$2HCrO_4^- + 3Fe^0 + 14H^+ \rightarrow 2Cr^{3+} + 3Fe^{2+} + 8H_2O$$

$$HCrO_4^- + 3Fe^{2+} + 7H^+ \rightarrow Cr^{3+} + 3Fe^{3+} + 4H_2O$$

Converted into units, when pH=2 and the initial concentration of Cr(VI) is 10 mg/L, the removal of Cr(VI) by the composite material with the dosage of 0.1 g/L is 81.4 mg/g.

Figure 4(c) shows the removal efficiency of CF-FeNPs composite material on Cr(VI). It can be seen from the figure that as the dosage of CF-FeNPs composite material increases, more reactive sites are correspondingly increased, and the removal efficiency of Cr(VI) shows an increasing trend (Karimi-Maleh et al. 2020; Wei et al. 2017). In the early stage of the reaction, high material reactivity has more active sites to participate in the reaction. In the late stage of the reaction, the composite material is passivated and adsorbed on the surface of the material, thereby reducing the active sites of the reaction. The pollutant loses the opportunity to contact the material, and the transfer of electrons is therefore hindered, causing the removal rate to not be continuously and effectively improved. When the dosage reaches 0.2 g/L, Cr(VI) in the solution can be basically removed after 2 h. In the follow-up experiment, based on the consideration of economic cost, we used CF-FeNPs composite material with a dosage of 0.2 g/L for investigation.

The effect of different initial Cr(VI) concentrations (10-30 mg/L) on the removal efficiency is shown in Figure 4(d). With the increase of the initial Cr(VI) solution concentration, the removal rate of CF-FeNPs composites also decreased. When the concentration of Cr(VI) solution is 10 mg/L, the removal rate within 4 h is 99.4%. When the concentration of Cr(VI) solution is 20 mg/L, the removal rate is 72.4%. When the concentration of Cr(VI) solution is 30 mg/L, the removal rate is 53.7%. A certain amount of CF-FeNPs means that the effective surface of the material is certain, that is, the surface active sites are limited (Xu et al. 2020; Ying et al. 2020; Zhang et al. 2020a, 2020b). Since the Cr(VI) is transferred to the surface of nanoparticles through competitive adsorption, the increasing concentration of Cr(VI) in the solution reduces the contact probability between the Cr(VI) ions and nanoparticles. This results in a part of Cr(VI) unable to contact the surface active sites of the CF-FeNPs composite material, thereby reducing the removal rate.

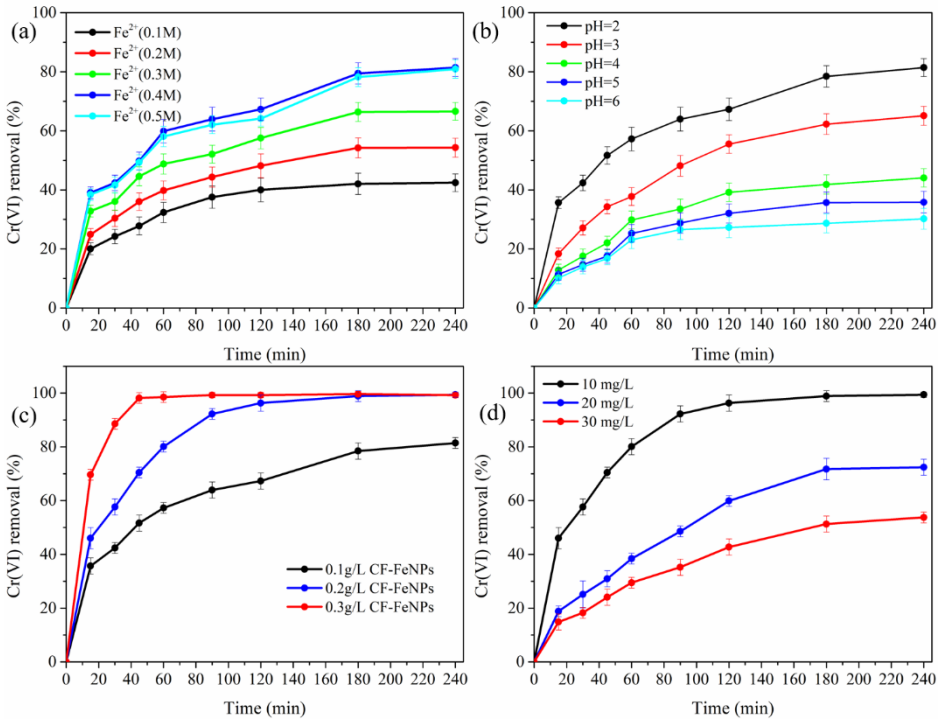

FIGURE 4. (a) The effect of different Fe^{2+} concentrations on the removal of Cr(VI) (the initial Cr(VI) concentration is 10 mg/L, dosage of CF-FeNPs is 0.1 g/L, solution pH=2.0); (b) The effect of different pHs on the remove Cr (VI) (initial Cr(VI) concentration is 10 mg/L, Fe^{2+} concentration is 0.4 M, CF-FeNPs dosage is 0.1g/L); (c) The influence of different dosages on the removal of Cr(VI) (the initial concentration of Cr(VI) is 10 mg/L, the concentration of Fe^{2+} is 0.4 M, solution pH=2.0); (d) The effect of different initial concentrations on the removal of Cr(VI) (Fe^{2+} concentration is 0.4 M, the dosage of CF-FeNPs is 0.2 g/L , solution pH=2.0, n=3)

The effect of the stability of CF-FeNPs composite material on the Cr(VI) removal efficiency is shown in Figure 5. Within half a month, with the increase of the CF-FeNPs composite material's parking time, the removal efficiency of Cr(VI) is slowly decreasing, and the material removal efficiency is reduced by 9%.

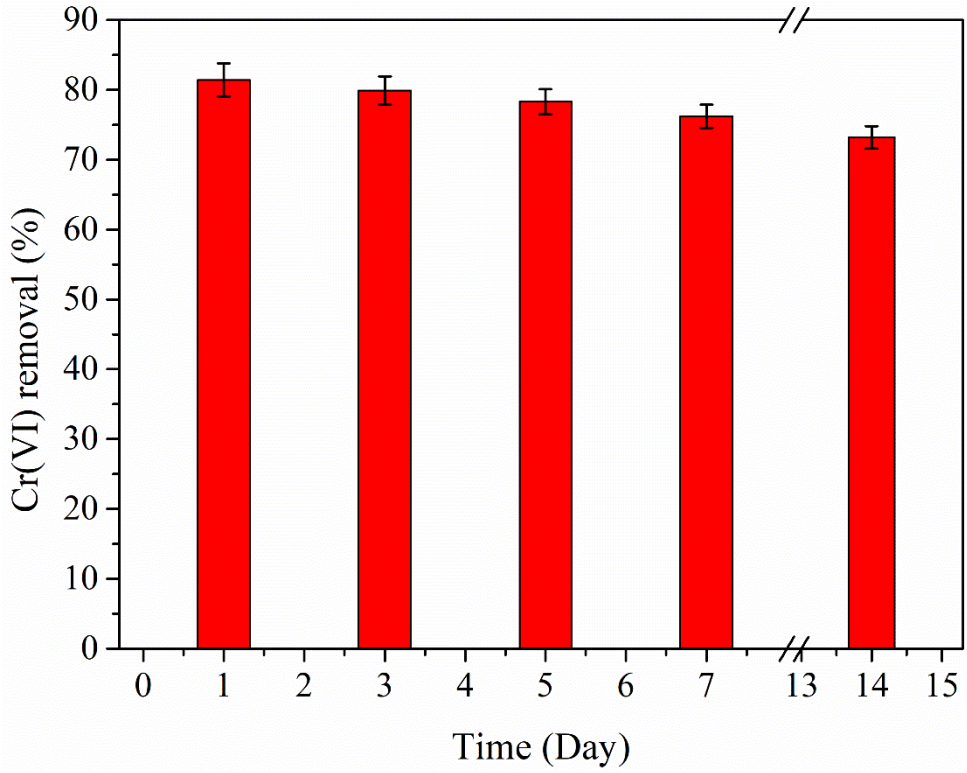

FIGURE 5. Influence of stability performance (initial Cr(VI) concentration is 10 mg/L, amount of CF-FeNPs is 0.1g/L, solution pH=2.0, n=3)

The pseudo-first-order kinetic model is used to describe the kinetic characteristics of the removal of Cr(VI) from water by the CF-FeNPs composite material under the experimental design more accurately. This shows that chemical adsorption is the rate-limiting step in this reaction, and adsorption is a mass transfer process. The chemical reaction in this process is also controlled by other mechanisms, such as internal and external particle diffusion, complexes, and ion exchange (Paunovic et al. 2020; Shalaby & Mohamed 2020).

The fitting results of the pseudo first-order kinetics are shown in Figure 6. The calculations in this figure correspond to Figure 4. As shown in Figure 6(a), as the initial concentration of Fe^{2+} increases, the corresponding reaction rate increases from 0.0028 min^{-1} (0.1 M Fe^{2+}) to 0.00658 min^{-1} (0.1 M Fe^{4+}). Figure 6(b) shows the effect of solution pH. When the pH is 2 and the dosage is 0.1 g/L, the largest rate constant and the highest removal rate are 0.00658 min^{-1} and 81.4%, respectively. However, when the pH rises to 6, the rate constant k_{obs} decreases to 0.0239 min^{-1}. Figure 6(c) shows the effect of dosage. The reaction rate constant shows a trend that increases with the increase of dosage. When the dosage is 0.3 g/L, it corresponds to 0.0471 min^{-1}. The results of the kinetic fitting corresponding to the concentration changes are shown in Figure 6(d), and the corresponding reaction rate constants are 0.0182, 0.00669, and 0.00365 min^{-1}. Through kinetic analysis, the prepared CF-FeNPs composite material has a good removal efficiency for a lower concentration of Cr(VI) solution under acidic conditions.

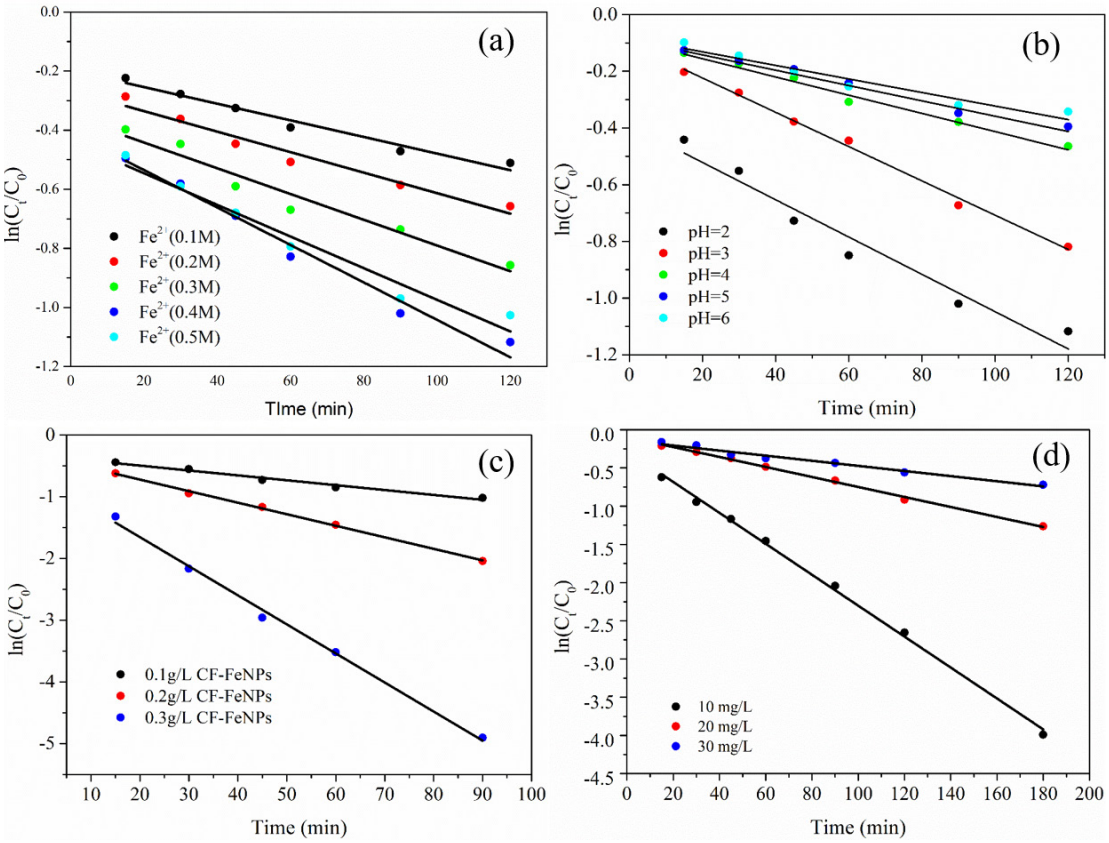

FIGURE 6. Pseudo first-order kinetic fitting results of different (a) Fe^{2+} concentration; (b) initial pH of solution; (c) dosage; and (d) Cr(VI) initial concentration

CONCLUSION

Under the experimental conditions of this study, increasing the Fe^{2+} concentration and the dosage of composite materials, while keeping the low initial concentration and pH value, is beneficial to the removal of Cr(VI) by CF-FeNPs composite. The removal rate of Cr(VI) by the CF-FeNPs composite can reaches 81.4% when the pH and initial concentration of Cr(VI) were 2 and 10 mg/L within 2 h, respectively. Under the optimal reaction conditions, the mechanism of removing Cr(VI) using CF-FeNPs composite can be summarized as a complex and coexisting reduction-coupled adsorption co-precipitation process. The FeNPs loaded on CF can be recommended for wastewater treatment.

ACKNOWLEDGEMENTS

This work was funded by The National Key Research and Development Program of China (2017YFD0202100).

REFERENCES

Bae, S., Gim, S., Kim, H. & Khalil, H. 2016. Effect of NaBH4 on properties of nanoscale zero-valent iron and its catalytic activity for reduction of p-nitrophenol. *Applied Catalysis B: Environmental* 182: 541-549.

Banerjee, M., Basu, R.K. & Das, S.K. 2018. Cr (VI) adsorption by a green adsorbent walnut shell: Adsorption studies, regeneration studies, scale-up design and economic feasibility. *Process Safety and Environmental Protection* 116: 693-702.

Batool, R., Kim, Y. & Shahida Hasnain. 2012. Hexavalent chromium reduction by bacteria from tannery effluent. *J. Microbiol. Biotechnol.* 22(4): 547-554.

Chavan, R.R., Bhinge, S.D., Bhutkar, M.A., Randive, D.S., Wadkar, G.H., Todkar, S.S. & Urade, M.N. 2020. Characterization, antioxidant, antimicrobial and cytotoxic activities of green synthesized silver and iron nanoparticles using alcoholic *Blumea eriantha* DC plant extract. *Materials Today Communications* 24: 101320.

Chen, A., Shang, C., Shao, J., Zhang, J. & Huang, H. 2017. The application of iron-based technologies in uranium remediation: A review. *Science of The Total Environment* 575: 1291-1306.

Clementino, M., Shi, X. & Zhang, Z. 2018. Oxidative stress and metabolic reprogramming in Cr (VI) carcinogenesis. *Current Opinion in Toxicology* 8: 20-27.

Dermentzis, K., Valsamidou, E. & Marmanis, D. 2012. Simultaneous removal of acidity and lead from acid lead battery wastewater by aluminum and iron electrocoagulation. *Journal of Engineering Science & Technology Review* 5(2): 1-5.

Dong, H., Zeng, Y., Zeng, G., Huang, D., Liang, J., Zhao, F., He, Q., Xie, Y. & Wu, Y. 2016. EDDS-assisted reduction of Cr (VI) by nanoscale zero-valent iron. *Separation and Purification Technology* 165: 86-91.

Ebrahiminezhad, A., Zare-Hoseinabadi, A., Sarmah, A.K., Taghizadeh, S., Ghasemi, Y. & Berenjian, A. 2018. Plant-mediated synthesis and applications of iron nanoparticles. *Molecular Biotechnology* 60(2): 154-168.

Fu, F., Ma, J., Xie, L., Tang, B., Han, W. & Lin, S. 2013. Chromium removal using resin supported nanoscale zero-valent iron. *Journal of Environmental Management* 128: 822-827.

Fu, L., Xie, K., Wang, A., Lyu, F., Ge, J., Zhang, L., Zhang, H., Su, W., Hou, Y.L., Zhou, C., Wang, C. & Ruan, S. 2019. High selective detection of mercury (II) ions by thioether side groups on metal-organic frameworks. *Analytica Chimica Acta* 1081: 51-58. https://doi.org/10.1016/j.aca.2019.06.055.

Gautam, A., Rawat, S., Verma, L., Singh, J., Sikarwar, S., Yadav, B.C. & Kalamdhad, A.S. 2018. Green synthesis of iron nanoparticle from extract of waste tea: An application for phenol red removal from aqueous solution. *Environmental Nanotechnology, Monitoring & Management* 10: 377-387.

Ghanim, D., Al-Kindi, G.Y. & Hassan, A.K. 2020. Green synthesis of iron nanoparticles using black tea leaves extract as adsorbent for removing eriochrome blue-black B dye. *Engineering and Technology Journal* 38(10A): 1558-1569.

Huang, L., Weng, X., Chen, Z., Megharaj, M. & Naidu, R. 2014. Green synthesis of iron nanoparticles by various tea extracts: Comparative study of the reactivity. *Spectrochimica Acta Part A: Molecular and Biomolecular Spectroscopy* 130: 295-301.

Janghel, E.K., Rai, M.K., Gupta, V.K. & Rai, J.K. 2007. Trace spectrophotometric determination of dichlorvos using diphenyl semicarbazide (DPC) in environmental and agricultural samples. *Journal of the Chinese Chemical Society* 54(2): 345-350.

Jing, C., Li, Y.L. & Landsberger, S. 2016. Review of soluble uranium removal by nanoscale zero valent iron. *Journal of Environmental Radioactivity* 164: 65-72.

Kalidhasan, S., Krishna Kumar, A.S., Rajesh, V. & Rajesh, N. 2013. Enhanced adsorption of hexavalent chromium arising out of an admirable interaction between a synthetic polymer and an ionic liquid. *Chemical Engineering Journal* 222: 454-463.

Karimi-Maleh, H., Alizadeh, M., Orooji, Y., Karimi, F., Baghayeri, M., Rouhi, J., Tajik, S., Beitollahi, H., Agarwal, S., Gupta, V.K., Rajendran, S., Rostamnia, S., Fu, L., Saberi-Movahed, F. & Malekmohammadi, S. 2021a. Guanine-based DNA biosensor amplified with Pt/SWCNTs nanocomposite as analytical tool for nanomolar determination of daunorubicin as an anticancer drug: A docking/experimental investigation. *Industrial & Engineering Chemistry Research* 60(2): 816-823. https://doi.org/10.1021/acs.iecr.0c04698.

Karimi-Maleh, H., Ayati, A., Davoodi, R., Tanhaei, B., Karimi, F., Malekmohammadi, S., Orooji, Y., Fu, L. & Sillanpää, M. 2021b. Recent advances in using of chitosan-based adsorbents for removal of pharmaceutical contaminants: A review. *Journal of Cleaner Production* 291: 125880. https://doi.org/10.1016/j.jclepro.2021.125880.

Karimi-Maleh, H., Orooji, Y., Ayati, A., Qanbari, S., Tanhaei, B., Karimi, F., Alizadeh, M., Rouhi, J., Fu, L. & Sillanpää, M. 2020. Recent advances in removal techniques of Cr(VI) toxic ion from aqueous solution: A comprehensive review. *Journal of Molecular Liquids* 2020: 115062. https://doi.org/10.1016/j.molliq.2020.115062.

Koushkbaghi, S., Zakialamdari, A., Pishnamazi, M., Ramandi, H.F., Aliabadi, M. & Irani, M. 2018. Aminated-Fe3O4 nanoparticles filled chitosan/PVA/PES dual layers nanofibrous membrane for the removal of Cr (VI) and Pb (II) ions from aqueous solutions in adsorption and membrane processes. *Chemical Engineering Journal* 337: 169-182.

Kumar, R., Anupama, A.V., Kumaran, V. & Sahoo, B. 2018. Effect of solvents on the structure and magnetic properties of pyrolysis derived carbon globules embedded with iron/iron carbide nanoparticles and their applications in magnetorheological fluids. *Nano-Structures & Nano-Objects* 16: 167-173.

Machado, S., Pinto, S.L., Grosso, J.P., Nouws, H.P.A., Albergaria, J.T. & Delerue-Matos, C. 2013. Green production of zero-valent iron nanoparticles using tree leaf extracts. *Science of The Total Environment* 445: 1-8.

Mashayekhi, F., Shafiekhani, A., Ali Sebt, S. & Darabi, E. 2018. The effect of initial pressure on growth of FeNPs in amorphous carbon films. *International Nano Letters* 8(1): 25-30.

Mehrotra, N., Tripathi, R.M., Zafar, F. & Singh, M.P. 2017. Catalytic degradation of dichlorvos using biosynthesized zero valent iron nanoparticles. *IEEE Transactions on Nanobioscience* 16(4): 280-286.

Mohan, D. & Pittman Jr. C.U. 2006. Activated carbons and low cost adsorbents for remediation of tri-and hexavalent chromium from water. *Journal of Hazardous Materials* 137(2): 762-811.

Patel, D., Vithalani, R. & Modi, C.K. 2020. Highly efficient FeNP-embedded hybrid bifunctional reduced graphene oxide for knoevenagel condensation with active methylene compounds. *New Journal of Chemistry* 44(7): 2868-2881.

Paunovic, J., Vucevic, D., Radosavljevic, T., Mandić-Rajčević, S. & Pantic, I. 2020. Iron-based nanoparticles and their potential toxicity: Focus on oxidative stress and apoptosis. *Chemico-Biological Interactions* 316: 108935.

Plachtová, P., Medrikova, Z., Zboril, R., Tucek, J., Varma, R.S. & Maršálek, B. 2018. Iron and iron oxide nanoparticles synthesized with green tea extract: Differences in ecotoxicological profile and ability to degrade malachite green. *ACS Sustainable Chemistry & Engineering* 6(7): 8679-8687.

Qian, A., Liao, P., Yuan, S. & Luo, M. 2014. Efficient reduction of Cr (VI) in groundwater by a hybrid electro-Pd process. *Water Research* 48: 326-334.

Shalaby, A.A. & Mohamed, A.A. 2020. Sensitive assessment of hexavalent chromium using various uniform and non-uniform color space signals derived from digital images. *Water, Air, & Soil Pollution* 231(10): 1-10.

Sun, Q., Hu, X., Zheng, S., Zhang, J. & Sheng, J. 2019. Effect of calcination on structure and photocatalytic property of N-TiO2/g-C3N4@ diatomite hybrid photocatalyst for improving reduction of Cr (VI)'. *Environmental Pollution* 245: 53-62.

Wang, Q., Huang, L., Pan, Y., Quan, X. & Puma, G.L. 2017. Impact of Fe (III) as an effective electron-shuttle mediator for enhanced Cr (VI) reduction in microbial fuel cells: Reduction of diffusional resistances and cathode overpotentials. *Journal of Hazardous Materials* 321: 896-906.

Wang, T., Jin, X., Chen, Z., Megharaj, M. & Naidu, R. 2014. Green synthesis of Fe nanoparticles using eucalyptus leaf extracts for treatment of eutrophic wastewater. *Science of The Total Environment* 466: 210-213.

Wang, W., Hu, B., Wang, C., Liang, Z., Cui, F., Zhao, Z. & Yang, C. 2020. 'Cr (VI) removal by micron-scale iron-carbon composite induced by ball milling: The role of activated carbon. *Chemical Engineering Journal* 389: 122633.

Wei, S., Li, D., Huang, Z., Huang, Y. & Wang, F. 2013. High-capacity adsorption of Cr (VI) from aqueous solution using a hierarchical porous carbon obtained from pig bone. *Bioresource Technology* 134: 407-411.

Wei, Y., Fang, Z., Zheng, L. & Tsang, E.P. 2017. Biosynthesized iron nanoparticles in aqueous extracts of *Eichhornia crassipes* and its mechanism in the hexavalent chromium removal. *Applied Surface Science* 399: 322-329.

Xu, Y., Lu, Y., Zhang, P., Wang, Y., Zheng, Y., Fu, L., Zhang, H., Lin, C-T. & Yu, A. 2020. Infrageneric phylogenetics investigation of chimonanthus based on electroactive compound profiles. *Bioelectrochemistry* 133: 107455. https://doi.org/10.1016/j.bioelechem.2020.107455.

Yin, Z., Liu, W., Bao, M. & Li, Y. 2021. Magnetic chitosan-based aerogel decorated with polydimethylsiloxane: A high-performance scavenger for oil in water. *Journal of Applied Polymer Science* 2021: 50461.

Ying, J., Zheng, Y., Zhang, H. & Fu, L. 2020. Room temperature biosynthesis of gold nanoparticles with *Lycoris aurea* leaf extract for the electrochemical determination of aspirin. *Revista Mexicana de Ingeniería Química* 19(2): 585-592.

Zeng, Q., Hu, Y., Yang, Y., Hu, L., Zhong, H. & He, Z. 2019. Cell envelop is the key site for Cr (VI) reduction by *Oceanobacillus oncorhynchi* W4, a newly isolated Cr (VI) reducing bacterium. *Journal of Hazardous Materials* 368: 149-155.

Zhang, H-Y., Wang, Y., Xiao, S., Wang, H., Wang, J-H. & Feng, L. 2017. Rapid detection of Cr (VI) ions based on cobalt (II)-doped carbon dots. *Biosensors and Bioelectronics* 87: 46-52.

Zhang, M., Pan, B., Wang, Y., Du, X., Fu, L., Zheng, Y., Chen, F., Wu, W., Zhou, Q. & Ding, S. 2020. Recording the electrochemical profile of *Pueraria* leaves for polyphyly analysis. *ChemistrySelect* 5(17): 5035-5040.

Zhang, X., Yang, R., Li, Z., Zhang, M., Wang, Q., Xu, Y., Fu, L., Du, J., Zheng, Y. & Zhu, J. 2020. Electroanalytical study of infrageneric relationship of *Lagerstroemia* using glassy carbon electrode recorded voltammograms. *Revista Mexicana de Ingeniería Química* 19(Sup. 1): 281-291.

Zhou, J., Zheng, Y., Zhang, J., Karimi-Maleh, H., Xu, Y., Zhou, Q., Fu, L. & Wu, W. 2020. Characterization of the electrochemical profiles of *Lycoris* seeds for species identification and infrageneric relationships. *Analytical Letters* 53(15): 2517-2528. https://doi.org/10.1080/00032719.2020.1746327.

Haobin Shi, Fei Chen, Li Fu* & Shichao Zhao
College of Materials and Environmental Engineering
Hangzhou Dianzi University
Hangzhou, 310018
P.R. China

Wenbin Zhang & Feng Chen
Xinchang Bureau of Agriculture and Rural Affairs
Shaoxing, 312500
P.R. China

Qingsheng Shi
Zhehua Xinnong (Jia Xing) Biotechnological Co., Ltd.
P.R. China

*Corresponding author; email: fuli@hdu.edu.cn

Received: 25 January 2021
Accepted: 4 March 2021